scientific reports

Check for updates

OPEN

Clinical impacts of *Artocarpus lakoocha* agglutinin-binding glycans for prognosis and treatment of cholangiocarcinoma

Phisit Sintusen[1], Kulthida Vaeteewoottacharn[1,2], Ubon Cha'on[1], Chawalit Pairojkul[3], Chaiwat Aphivatanasiri[3], Sutas Suttiprapa[4], Panupong Mahalapbutr[1,2], Atit Silsirivanit[1,2], Sopit Wongkham[1,2] & Sukanya Luang[1,2]✉

Artocarpus lakoocha **agglutinin (ALA), which specifically targets the Gal/GalNAc components of complex glycans, was isolated from the seeds of *Artocarpus lakoocha*. This study is the first to explore the role of ALA in identifying aberrant glycans, designated ALA-binding glycans (ALAG), and its implications in cholangiocarcinoma (CCA). ALA-histochemistry was used to evaluate ALAG expression in liver fluke-induced CCA tissues from hamsters ($n = 60$). Elevated ALAG expression was observed in hyperplastic ducts and significantly increased in CCA tissues, while normal biliary epithelium and hepatocytes showed no expression. Similar results were found in patient CCA tissues ($n = 68$), where higher ALAG levels correlated with shorter survival rates, indicating the involvement of ALAG in CCA development and progression. Furthermore, ALA treatment inhibited cell viability in CCA cell lines, as demonstrated by MTT and colony formation assays, and Ki-67 expression. ALA treatment also decreased cell migration and invasion, as shown by Transwell assays. Gelatin zymography suggested that these effects might be associated with reduced MMP-9 activity. Overall, these findings may position ALAG as a potential marker for poor prognosis in CCA, while ALA may serve as a novel lectin for both detection and therapeutic applications in CCA.**

Keywords *Artocarpus lakoocha* agglutinin, Cholangiocarcinoma, Aberrant glycosylation, T and Tn antigens, Anti-metastasis, Anti-proliferation

Abbreviations

CCA	Cholangiocarcinoma
ALA	*Artocarpus lakoocha* Agglutinin
ALAG	ALA-binding glycans
Ov	*Opisthorchis viverrini*
NDMA	N-nitrosodimethylamine
HP	Hyperplastic ducts
NBD	Normal bile ducts
Gal	Galactose
GalNAc	N-acetylgalactosamine
BSM	Bovine submaxillary mucin

Cholangiocarcinoma (CCA) is a malignant tumor originating from the epithelial cells of the bile ducts. A major risk factor for developing CCA in Asia, particularly in northeastern Thailand, is a chronic infection with liver flukes (*Opisthorchis viverrini*, Ov)[1,2]. The persistent inflammation caused by these infections can expose the bile duct epithelium to carcinogenic substances, leading to genetic and epigenetic changes that may result in CCA[3]. CCA is characterized by its aggressive behavior and unfavorable prognosis, as it is frequently diagnosed at advanced stages due to its nonspecific and ambiguous symptoms. The stage of diagnosis significantly impacts

[1]Department of Biochemistry, Faculty of Medicine, Khon Kaen University, Khon Kaen 40002, Thailand. [2]Center for Translational Medicine, Faculty of Medicine, Khon Kaen University, Khon Kaen 40002, Thailand. [3]Department of Pathology, Faculty of Medicine, Khon Kaen University, Khon Kaen 40002, Thailand. [4]Department of Tropical Medicine, Faculty of Medicine, Khon Kaen University, Khon Kaen 40002, Thailand. ✉email: sukany@kku.ac.th

prognosis, emphasizing the need for early detection to improve patient outcomes[4–6]. Therefore, ongoing research focused on developing methods for early detection, predicting prognosis, and targeted therapies is essential for improving patient outcomes.

The progression of CCA is frequently associated with changes in glycosylation, which is the process of modifying sugars on the proteins or lipids. The expression of abnormal glycans in CCA can influence tumor behavior and patient outcomes[7–9]. Altered glycan structures affect cell signaling leading to enhancing the capabilities of cancer cells in tumor growth, migration, invasion, and avoiding the immune system[10–15]. High expression of O-truncated glycans, specifically Tn (N-acetylgalactosamine; GalNAc)- and T (GalNAc-galactose; GalNAc-Gal) antigens, has been reported in various cancers, including colorectal, pancreatic, breast, gastric, and lung cancers[16–22]. The altered glycans have the potential to serve as biomarkers for diagnosis and prognosis, while also being critical in tumor biology by influencing cancer cell behavior and their interactions with the tumor microenvironment[18,23,24].

Lectins are carbohydrate-binding proteins or glycoprotiens that are crucial in various biological processes such as cell–cell recognition, signaling, and immune responses[25]. They are particularly valuable in medical glycosciences due to their ability to selectively bind to specific glycan structures on cell surfaces. This property makes lectins useful for studying aberrant glycosylation patterns associated with different diseases, including cancers. Using various plant lectins with different sugar-binding specificities, N-acetylglucosamine (GlcNAc), GalNAc, and terminal fucose were demonstrated to be aberrantly expressed in patient-CCA tissues[26]. Suppression of N-acetylgalactosaminyltransferases, the enzyme that transfers the first GalNAc sugar of O-glycosylation in CCA cell lines, significantly reduced proliferation, migration, and invasion of CCA cells[27,28]. These findings indicate the significance of GalNAc/GalNAc-Gal glycans in the development and progression of CCA.

Artocarpus lakoocha agglutinin (ALA) is a plant lectin isolated from seeds of *A. lakoocha*[29]. ALA exhibits agglutinin activity and has a preference for binding to T- and Tn-associated glycoproteins and monosaccharides such as Gal and GalNAc[29,30]. ALA exhibited antiproliferative effects on leukemic cells and could serve as a sensitive tool to differentiate leukemic cell lines from normal lymphocytes[31]. In this study, we evaluated the ability of ALA to detect aberrant glycans designated as ALA-binding glycans (ALAG) in CCA. The importance of ALAG expression in CCA development, and the inhibitory effects of ALA on growth, and progression of CCA were demonstrated.

Results

ALAG expression is elevated in human CCA tissues

The purified ALA was biotinylated and utilized to detect ALAG expression in human CCA tissues (Supplementary Fig. S1). The expression of ALAG was determined in 68 liver sections from patients diagnosed with CCA using ALA-histochemistry (Fig. 1). ALAG expression was absent in hepatocytes and normal bile ducts (NBD) presented in non-tumor adjacent areas (Fig. 1A). In contrast, a positive signal of ALAG was identified in hyperplastic ducts (HP) ($n=35$), and peribiliary glands. Notably, ALAG was highly observed in the CCA regions across all 68 cases, with strong signals detected in the apical surface. To quantify the intensity (Fig. 1B) and frequency of ALAG expression, an ALAG-score was created, which facilitated the analysis of its correlation with the clinicopathological data of CCA patients. The ALAG expression was gradually increased from NBD, HP to CCA with the mean ALAG-score for NBD area $=8.03\pm10.6$, HP $=54.86\pm57.1$, and CCA $=118.97\pm53.7$ (Fig. 1C). The ALAG-scores were divided into four groups: negative (0), low (0–100), medium (101–200), and high (201–300). As shown in Fig. 1D, among 66 NBD examined, over 50% of NBD had negative ALAG, and the rest had low ALAG, while most HP had low ALAG with 17% HP expressing medium to high ALAG. In contrast, 62% of CCA areas exhibited medium to high ALAG-score. These observations implied the association of ALAG with CCA development.

High ALAG expression is associated with short survival of CCA patients

The association between ALAG expression and patient survival was evaluated using a Kaplan–Meier curve along with Log-rank analysis (Fig. 1E). In this cohort, the overall median survival for CCA patients was 209 days (95% CI, 148–269 days) with the median ALAG-score for CCA was 120, which served as the cut-off value to divide patients into two groups. Patients with high ALAG expression had a median survival of 180 days (95% CI, 101–258 days), while those with low ALAG expression had a median survival of 236 days (95% CI, 148–269 days). Patients with high ALAG expression demonstrated a significantly shorter survival rate compared to those with low ALAG-score. Additionally, there was no significant association between the ALAG-score and clinicopathological data, including sex, age, tumor size, histological types, and tumor stages (Table 1). Univariate and multivariate Cox regression analysis indicated that histological type and ALAG expression were independent prognostic factors for overall survival in CCA patients (Tables 2, 3).

High expression of ALAG is associated with CCA development in hamster model

ALA-histochemistry of CCA-induced hamster tissues was analyzed for ALAG expression across four groups of hamsters: untreated, Ov-infected, N-nitrosodimethylamine (NDMA)-treated, and Ov + NDMA-treated (CCA) groups (Fig. 2). No ALAG expression was detected in NBD from the four groups. However, ALAG signals were observed in HP in almost all groups (Fig. 2A and Table 4). Notably, the Ov + NDMA combination treatment revealed areas of CCA in the liver tissues, with ALAG expression increasing in correlation with the treatment duration (Fig. 2A). ALAG-score in NBD, HP, and CCA regions were quantified. As illustrated in Fig. 2B, ALAG expression was significantly higher in HP (mean $=61.0\pm22.3$) and CCA regions (mean $=105.5\pm26.7$) compared to NBD areas ($p<0.001$), indicating a potential role for ALAG in the development of CCA.

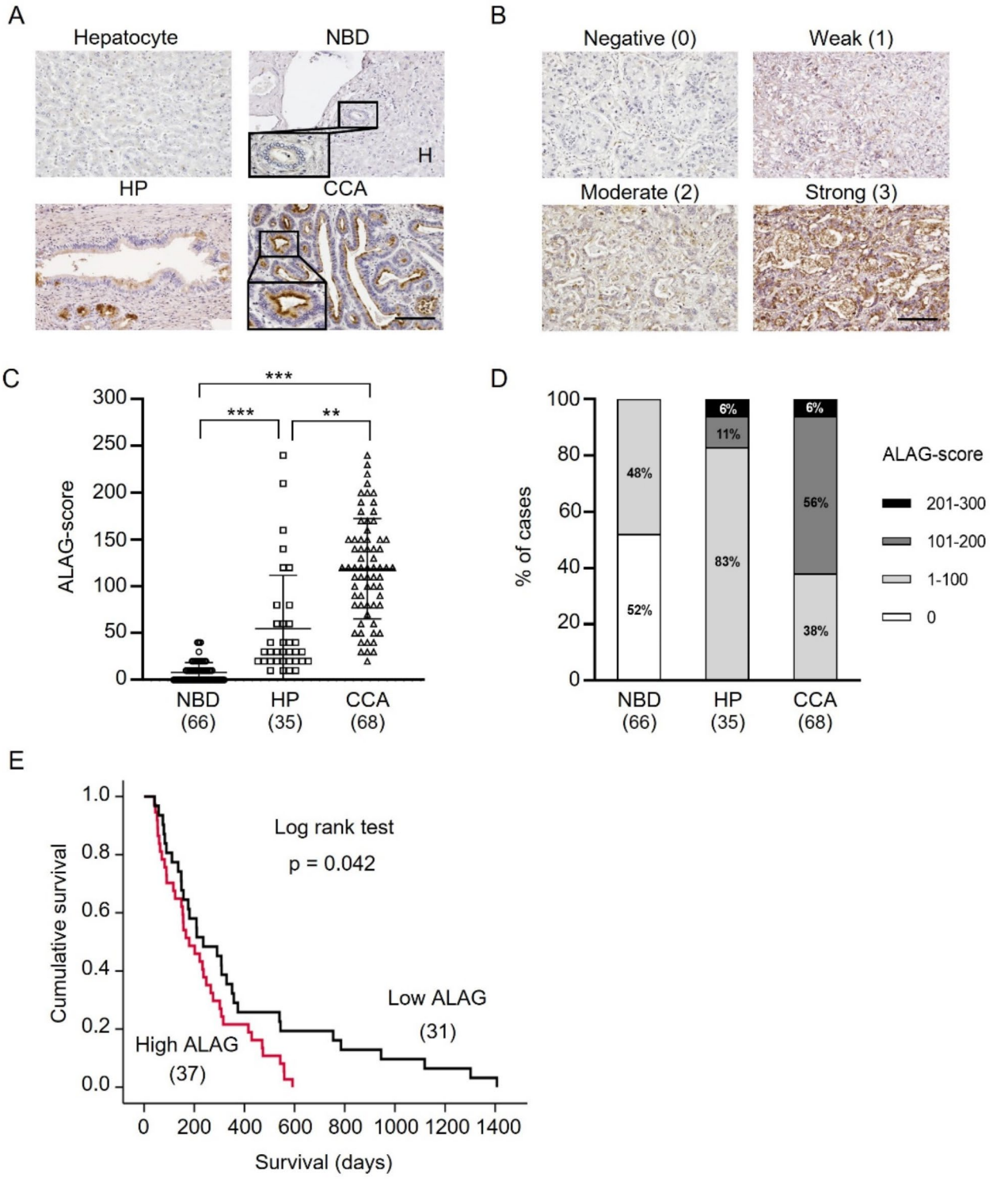

Fig. 1. Expression of ALAG in CCA patient tissues. (**A**) ALA-histochemical staining of CCA tissues. H, hepatocytes; NBD, normal bile ducts; HP, hyperplastic ducts; CCA, cholangiocarcinoma. The scale bar represents 100 µm. (**B**) Differential expression of ALAG in CCA tissues and intensity grading. The scale bar represents 100 µm. (**C**) Scatter plots depicting the ALAG-score in NBD, HP, and CCA. ** = $p < 0.01$, *** = $p < 0.001$. (**D**) The bar graph represents the percentage of CCA cases exhibiting a differential ALAG-score. The total number of cases is indicated in parentheses. (**E**) Survival analysis of CCA patients using Log-rank test and Kaplan–Meier plot. The total number of cases is indicated in parentheses.

Variables	N	ALAG expression (H-score)		*p*-value
		< 120	≥ 120	
Sex				
Male	45	20	25	0.791
Female	23	11	12	
Age (years)				
< 56	34	13	21	0.223
≥ 56	34	18	16	
Tumor size (cm)				
< 7	31	17	14	0.161
≥ 7	37	14	23	
Histological types				
Papillary type	19	10	9	0.468
Non-papillary type	49	21	28	
Tumor stages				
I–III	23	9	14	0.445
IVA-IVB	45	22	23	

Table 1. Correlation of ALAG expression and clinicopathological data of CCA patients. *cm* centimeter.

Variables	N	HR	95%CI	*p*-value
Sex				
Male	45	1		
Female	23	0.863	(0.519–1.435)	0.571
Age (years)				
< 56	34	1		
≥ 56	34	1.167	(0.718–1.896)	0.534
Tumor size (cm)				
< 7	31	1		
≥ 7	37	0.942	(0.581–1.526)	0.808
Histological types				
Papillary type	19	1		
Non-papillary type	49	1.878	(1.038–3.397)	0.037*
Tumor stages				
I–III	23	1		
IVA-IVB	45	0.971	(0.584–1.616)	0.910
ALAGs expression				
< 120	31	1		
≥ 120	37	1.691	(1.012–2.828)	0.045*

Table 2. Univariate analysis using Cox regression of clinicopathological characteristics and ALAG expression. *cm* centimeter, *HR* hazard ratio.

ALAG is differentially expressed in CCA cell lines

The expression of ALAG in CCA cell lines was performed using non-permeabilized ALA-cytofluorescent staining. As shown in Fig. 3A and B, ALAG was presented on the cell membrane of CCA cells, with particularly strong signals in KKU-100 and KKU-213B cell lines. In contrast, permeabilized ALA-cytofluorescent staining revealed that ALAG localized to the perinuclear region, with robust signals in KKU-100 and KKU-213B, while KKU-055 and KKU-213A exhibited weaker signals (Supplementary Fig. S2). To verify that the signal was a result of the interaction between ALA and ALAG, the activity of ALA was neutralized with glucose, Gal, GalNAc, and bovine submaxillary mucin (BSM). The signals were eliminated in cells treated with ALA combined with Gal, GalNAc, or BSM but remained unaffected in those treated with ALA and glucose which was used as a negative control (Fig. 3C and D). These results indicated that ALA specifically recognizes and binds to ALAG in CCA cell lines, particularly to glycans containing Gal and GalNAc.

Variables	N	HR	95%CI	*p*-value
Sex				
Male	45	1		
Female	23	0.872	(0.516–1.475)	0.610
Age (years)				
< 56	34	1		
≥ 56	34	1.336	(0.805–2.218)	0.262
Tumor size (cm)				
< 7	31	1		
≥ 7	37	0.872	(0.531–1.433)	0.590
Histological types				
Papillary type	19	1		
Non-papillary type	49	1.850	(1.002–3.418)	0.049*
Tumor stages				
I–III	23	1		
IVA-IVB	45	1.052	(0.620–1.787)	0.850
ALAGs expression				
< 120	31	1		
≥ 120	37	1.698	(1.002–2.877)	0.049*

Table 3. Multivariate analysis using Cox regression of clinicopathological characteristics and ALAG expression. *cm* centimeter, *HR* hazard ratio.

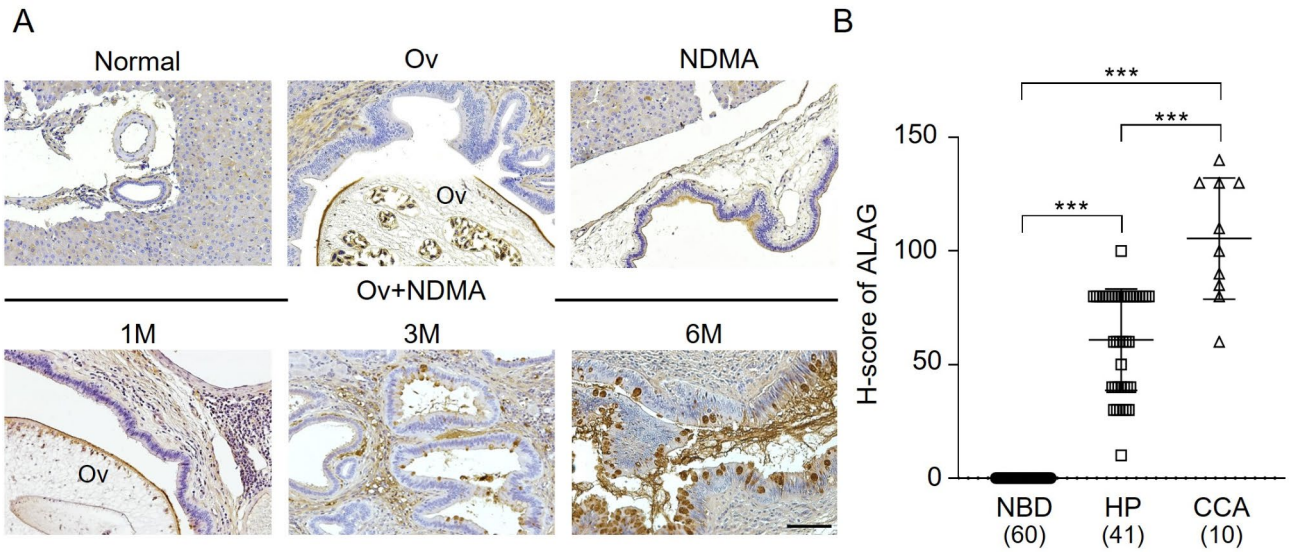

Fig. 2. Expression of ALAG in liver tissues of hamsters. (**A**) Expression of ALAG in bile ducts epithelium of liver tissues from normal (untreated), Ov (*Opisthorchis viverrini*-infected), NDMA (NDMA-treated) (upper panel), and Ov + NDMA (CCA group, lower panel) evaluated at 1, 3, and 6 months. The scale bar represents 100 μm. (**B**) The scatter plots display ALAG expression in mean ± SD of ALAG-score. Numbers in the parentheses indicate sample size. *** = $p < 0.001$.

ALA exerts inhibitory effects on growth and colony formation of CCA cell lines

First, the concentration of ALA that did not induce cell aggregation was examined. As shown in Supplementary Fig. S3, ALA at 5 to 30 μg/mL did not cause cell aggregation, and thus the cytotoxic effect of ALA at 5 to 30 μg/mL on CCA proliferation was subsequently assessed using the MTT assay. ALA significantly reduced cell viability of KKU-100 and KKU-213B in a dose-dependent manner, with approximately a 30% decrease observed at the highest concentration (Fig. 4A), whereas ALA treatment did not affect the viability of KKU-055 and KKU-213A. Analysis of the proliferation marker, Ki-67, showed a decrease in its expression following treatment with ALA (Fig. 4B and Supplementary Fig. S4). However, cell growth did not exhibit a time-dependent decline across all ALA concentrations (Fig. 4C). The cytotoxic effect of ALA on cell growth was further confirmed using colony forming assay. As shown in Fig. 5, ALA treatment significantly suppressed the growth of CCA cells.

Group of experiment	1M			3M			6M		
	NBD	HP	CCA	NBD	HP	CCA	NBD	HP	CCA
Untreated	0/5	–	–	0/5	–	–	0/5	–	–
Ov	0/5	5/5 (100)	–	0/5	5/5 (100)	–	0/5	5/5 (100)	–
NDMA	0/5	3/5 (60)	–	0/5	4/5 (80)	–	0/5	4/5 (80)	–
Ov + NDMA	0/5	5/5 (100)	–	0/5	5/5 (100)	5/5 (100)	0/5	5/5 (100)	5/5 (100)

Table 4. ALAG expression and histological classification in CCA-induced hamster tissues. All data are expressed as the number of ALAG-expressed cases/cases with the histological classification. The percentage of ALAG-positive cases is shown in parentheses. *NBD* normal bile duct, *HP* hyperplastic ducts, *CCA* cholangiocarcinoma.

ALA suppresses cell migration and invasion of CCA cell lines

The effect of ALA on the metastatic phenotype of CCA cell lines with high ALAG expression was investigated. Cells were treated with ALA 1–2 μg/mL, the concentration that did not affect cell viability. ALA significantly reduced the migration and invasion ability of KKU-100 and KKU-213B cells in a dose-dependent manner (Fig. 6A and B). Compared to the control, the percentage of migrated and invaded cells was significantly decreased following ALA treatment. Additionally, the effect of ALA on the enzymatic activities of MMP-2 and MMP-9 was evaluated using gelatin zymography, which revealed that ALA significantly decreased the activity of MMP-9 but not MMP-2 in KKU-100 and KKU-213B cells (Fig. 6C).

Discussion

In this research, ALA, a lectin that specifically targets tumor-associated T (Galβ1-3GalNAcα1-Ser/Thr), Tn (GalNAcα1-Ser/Thr) antigens, and Gal/GalNAc associated complex glycans, was successfully extracted and purified from the seeds of *A. lakoocha*. Initially, ALA was utilized to assess the levels of ALAG in CCA tissues and cell lines. The expression levels of ALAG were identified as being significantly correlated with the development and progression of CCA, and were also indicative of a poor prognosis for patients. Furthermore, treatment with ALA demonstrated the ability to inhibit the growth, migration, and invasion of CCA cells. These results suggest new opportunities for ALA and ALAG in therapeutic strategies and further pathophysiological investigations of CCA.

Using ALA-histochemistry in Ov-induced CCA hamster tissues, we observed a significant increase in ALAG expression during CCA development. While normal bile ducts and hepatocytes showed no ALAG expression, elevated levels were found in precancerous areas (hyperproliferative bile duct epithelial cells), and CCA itself. Similar results were noted in human CCA tissues. Moreover, the expression of ALAG was associated with different histological types and a reduced survival rate in CCA patients, highlighting the potential significance of ALAG expression in the progression and aggressiveness of CCA. Comparable observations were made with *Vicia villosa* lectin (VVL), which identifies GalNAc and GalNAc-Gal, indicating that these glycans were over-expressed in CCA, with levels rising progressively during carcinogenesis[27]. The increased presence of GalNAc and GalNAc-Gal (Tn and T antigens) may be a common feature in various cancers, as evidenced by similar findings across multiple cancer types[23,24,26,32,33].

Even though VVL and ALA recognize Gal and GalNAc, the two lectins may bind to different complexity of Gal/GalNAc-associated glycans. The assumption was based on the fact that the expression levels of VVL-binding glycans (VBG) and ALAG were different among the same CCA cell lines tested. Notably, VBG expression was particularly high in the KKU-213A (previously KKU-213) and KKU-213B (formerly KKU-214) cell lines, while lower signals were observed in KKU-055 and KKU-100. Conversely, ALA-cytofluorescent staining in this study indicated that ALAG was strongly expressed in KKU-100 and KKU-213B, but weakly expressed in KKU-055 and KKU-213A. It has been reported that VVL displays a strong affinity for the innermost GalNAc residue in O-GalNAcylated glycans, but not for GalNAc-elongated glycans[34]. In contrast, ALA identifies the Gal and GalNAc of the complex glycans[29–31]. These results imply that ALA is a novel lectin for investigating the complex glycans with Gal/GalNAc.

This report also provides the first evidence of the anti-proliferative activity of ALA in CCA. ALA treatment significantly decreased the viability of CCA cell lines with high ALAG expression, specifically KKU-100 and KKU-213B, in a dose-dependent manner (Figs. 4 and 5). The reduction of the proliferation marker, Ki-67, following ALA treatment supported the notion that ALA effectively inhibits cancer cell proliferation (Fig. 4B and Supplementary Fig. S4). These findings underscore ALAG could be considered as a potential target molecule for further exploration in CCA therapy. Moreover, the growth-inhibitory effect was prominently demonstrated in the colony formation assay, suggesting that prolonged treatment with ALA may be an effective strategy for managing CCA. Although the ALA-histochemistry analysis of human CCA tissues and CCA-induced hamster tissues revealed that normal bile duct epithelium and hepatocytes did not exhibit positive results for ALAG, further investigations using an animal model are necessary to assess the safety and specificity of ALA toxicity in CCA.

In addition to its cytotoxic effects, ALA demonstrated an inhibitory impact on cell migration and invasion. The migrated, and invaded cells of KKU-100 and KKU-213B were significantly reduced after ALA treatment (Fig. 6). These findings were corroborated by the study conducted by Detarya et al. (2020), which demonstrated that silencing GalNAc expression using siRNA targeting the GALNT5 enzyme significantly inhibited the

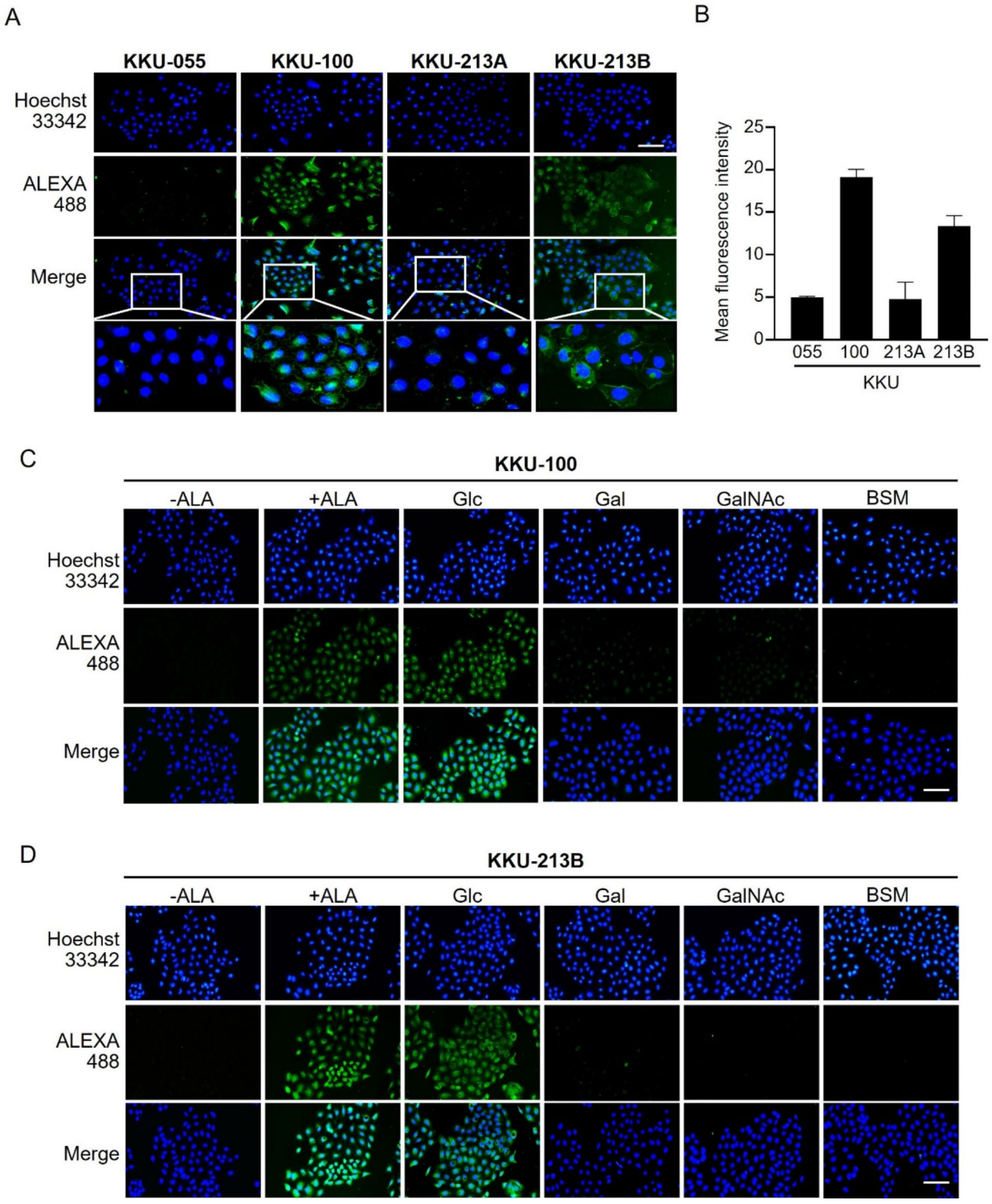

Fig. 3. ALAG expression in CCA cell lines. (**A**) Non-permeabilized ALA-cytofluorescent staining showed ALAG expression in the cytoplasm and on the cell membrane of CCA cell lines. (**B**) Mean fluorescent intensity of ALAG expression (mean ± SD) in each cell from three independent experiments. (**C**) A sugar inhibition test with permeabilized ALA-cytofluorescent staining. Cells were treated with ALA in the presence of glucose (Glc), galactose (Gal), N-acetylgalactosamine (GalNAc), and bovine submaxillary mucin (BSM) at 10 μg/mL, compared to those treated with ALA along (+ ALA) and without ALA (-ALA). The signal of Alexa-448 represents ALAG (green) and Hoechst33342 represents nuclear staining (blue). The scale bar represents 100 μm.

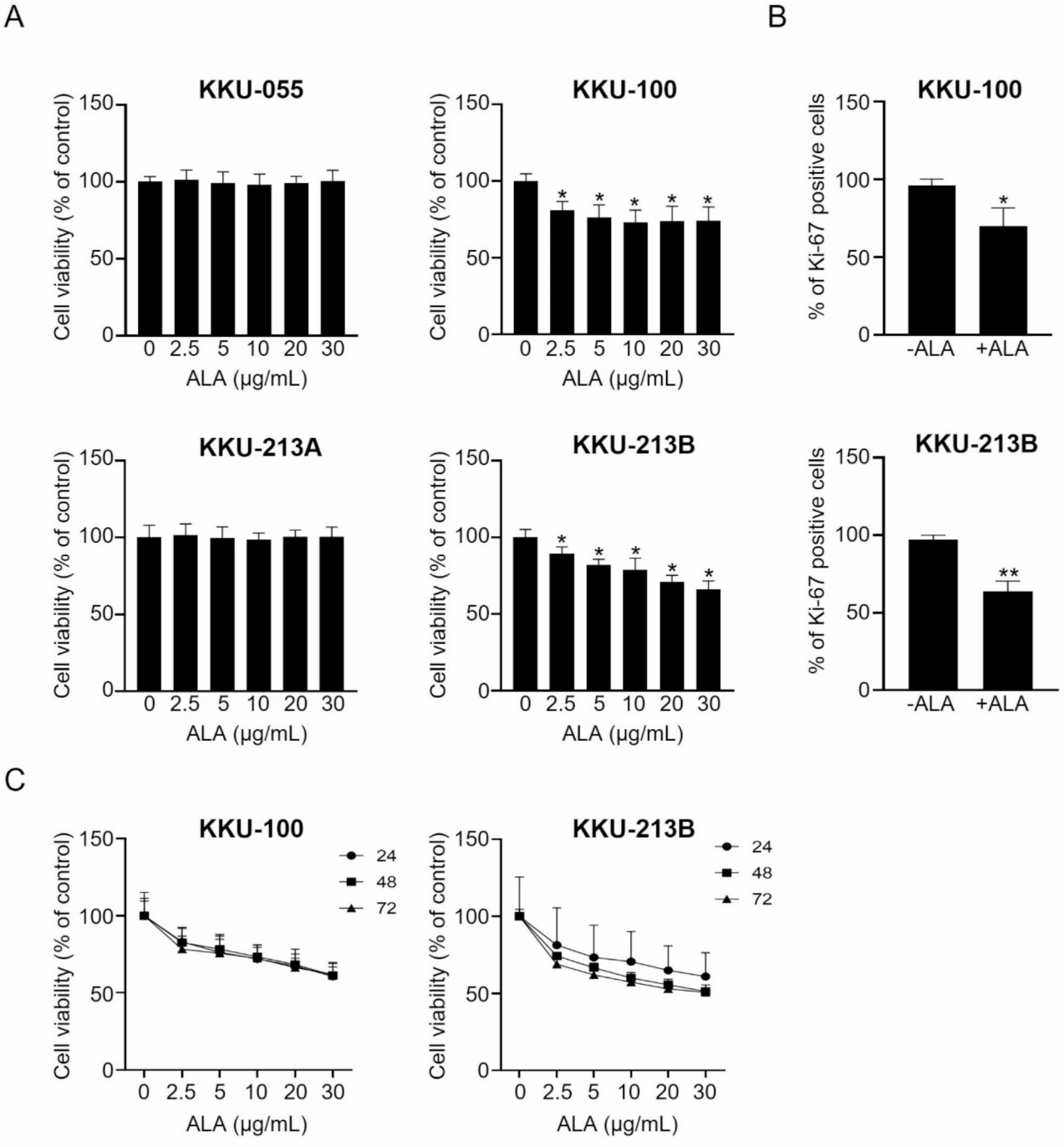

Fig. 4. Effect of ALA treatment on the viability of CCA cell lines. (**A**) Cell viability following exposure to ALA (2.5 to 30 μg/mL) for 24 h. The data presented are mean ± SD from three independent experiments. (**B**) Expression of proliferation marker Ki-67 in KKU-100 and KKU-213B after a 24-h incubation with 10 μg/mL of ALA. The data presented are mean ± SD from two independent experiments. (**C**) Cell viability of KKU-100 and KKU-213B after treatment with ALA (2.5–30 μg/mL) at 24, 48, and 72 h. Cells without ALA were used as a control. The data presented are mean ± SD from three independent experiments. * = $p < 0.05$, ** = $p < 0.01$.

migration and invasion of CCA cell lines. The mechanism is possible via the reduction of MMP-9 activity, as indicated by the zymography assay in our study. MMPs are essential for the degradation of the extracellular matrix, which facilitates tumor invasion and metastasis, as they help create and sustain an environment that facilitates the initiation and progression of both primary and metastatic tumors[35]. Further investigation is needed to explore the mechanisms underlying the effect of ALA on CCA cells, particularly regarding MMPs and the role of GALNTs on ALAG expression.

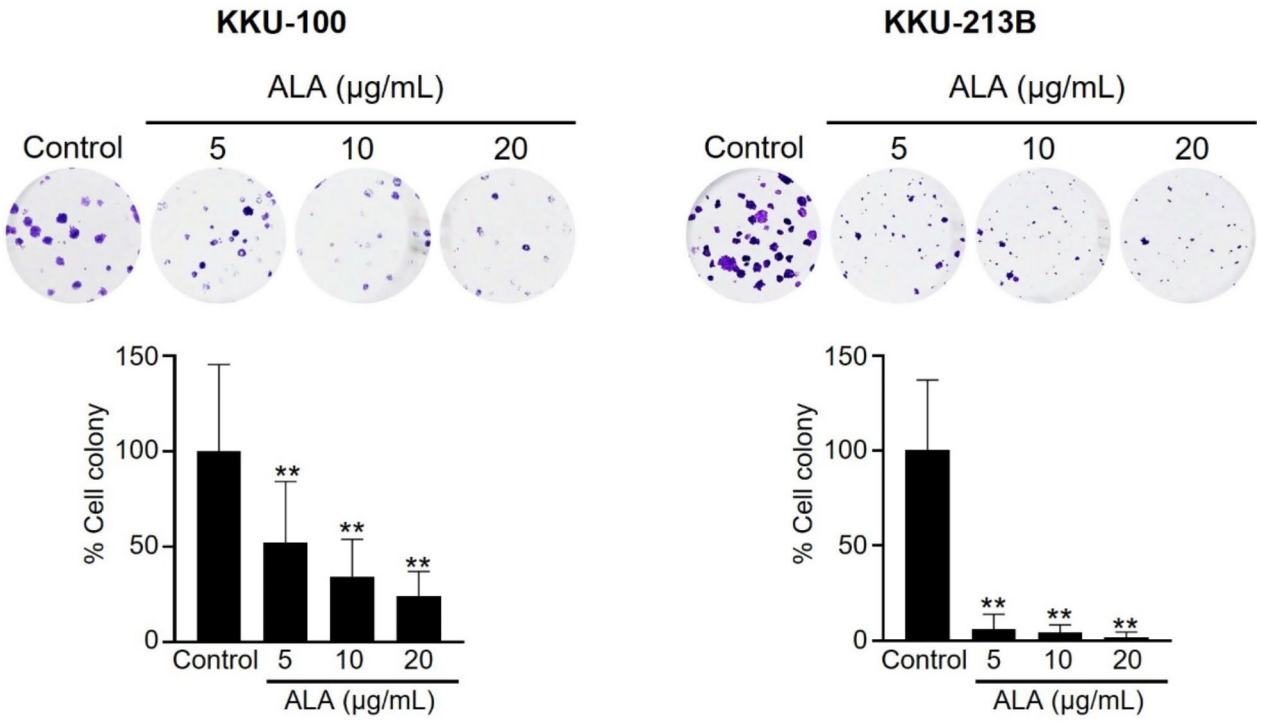

Fig. 5. Effect of ALA on cell viability using colony formation assay. KKU-100 and KKU-213B cells were treated with ALA (5 to 20 μg/mL) for 7 days, media with ALA replacing every three days. Bar graphs represent the number of colony formations after treatment with ALA. Error bars represent SD (** = $p < 0.01$ compared to control).

Conclusion

Lectins have become a focal point in cancer research due to their ability to recognize and bind specific glycan structures on glycoproteins and glycolipids. Changes in glycosylation can influence critical cellular processes, including proliferation, migration, and invasion in cancers. This study demonstrated for the first time that ALA plays a significant role in identifying tumor-associated glycans in CCA. ALA specifically targets the Gal and GalNAc components of complex glycans, which are essential during the early stages of CCA development. The correlation between elevated ALAG levels and poorer clinical outcomes in CCA patients suggests its potential as a prognostic marker. Additionally, ALA treatment effectively inhibited the proliferation, migration, and invasion of CCA cell lines with high ALAG expression. Future research should aim to clarify the mechanisms behind the alterations in Gal/GalNAc-associated glycans and their potential effects on cancer treatment strategies.

Materials and methods

ALA isolation and purification

ALA was purified as previously described[29]. Briefly, *Artocarpus lakoocha* seeds were ground into a fine powder and homogenized in 50 mM Tris–HCl buffer, pH 8.0. Protein precipitation was performed using ammonium sulfate fractionation. The precipitated protein from the 40–80% saturation fraction was collected and then resuspended in 50 mM Tris–HCl buffer, pH 8.5. The resuspended protein was dialyzed against the same buffer, at 4 °C overnight. The dialyzed protein was then subjected to a Q-Sepharose Fast Flow column and eluted with a gradient of NaCl from 0 to 1 M in 50 mM Tris–HCl buffer, pH 8.5. The purity of ALA was determined by SDS-PAGE[36]. Finally, the purified ALA was biotinylated using the EZ-Link™ Sulfo-NHS-LC-Biotinylation kit according to the manufacturer's instructions (Thermo Scientific; Waltham, MA).

Human CCA tissues

Tumor tissue samples were collected from Thai patients diagnosed with intrahepatic CCA. The formalin-fixed paraffin-embedded specimens were obtained from the Bio-bank of the Cholangiocarcinoma Research Institute, Khon Kaen University, Thailand. Informed consents were obtained from all patients and the research protocol has been reviewed and approved by the Ethics Committee for Human Research of Khon Kaen University, in accordance with the Declaration of Helsinki (HE661279).

CCA-induced hamster tissues

Formalin-fixed paraffin-embedded liver tissues from hamsters were obtained from previous experiments and categorized into four groups: untreated normal control, Ov-infected, NDMA-treated, and Ov + NDMA-treated

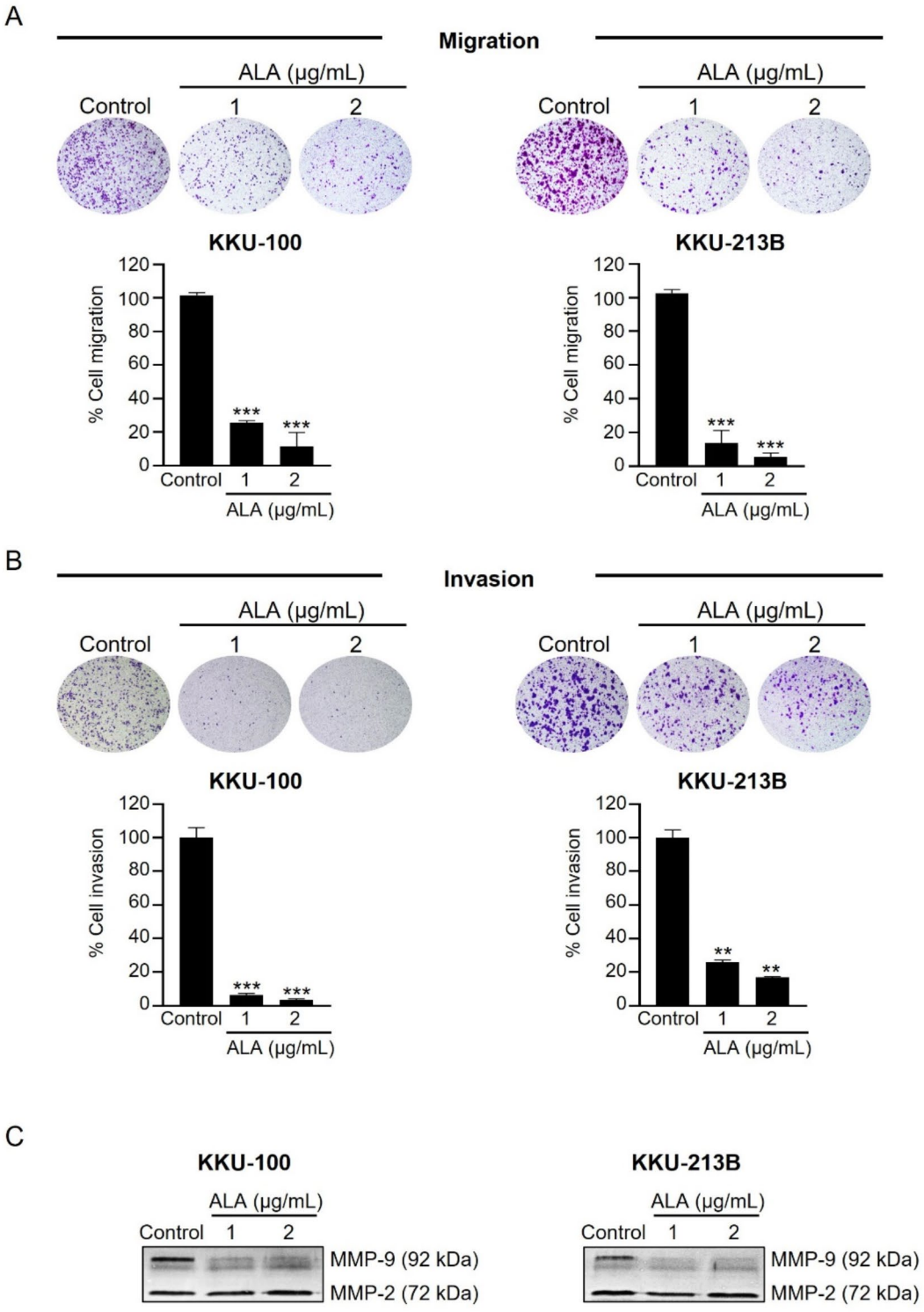

Fig. 6. Effect of ALA on migration and invasion of CCA cells. Cells were treated with ALA (1–2 μg/mL) for 24 h before subjecting to migration and invasion assays. Cells without ALA treatment were used as a control. (**A**) Migrated cells and (**B**) invaded cells were stained with 0.5% (w/v) crystal violet and observed under a microscope. The percentage of migrated and invaded cells was quantified and normalized with control. The data presented are mean ± SD from three independent experiments. ** = $p < 0.01$, *** = $p < 0.001$. (**C**) Gelatin zymography of MMP-2 and MMP-9 activities in the conditioned medium from KKU-100 and KKU-213B after 24 h of ALA treatment. The zymogram represents one of the three independent experiments.

groups. Animals in each group ($n=5$) were sacrificed at 1-, 3-, and 6-months post-treatment, as previously described[37]. All procedures were performed in accordance with the relevant guidelines and regulations, and the ARRIVE guidelines. The study protocol received approval from the Ethics Committee for Animal Research at Khon Kaen University (AEMDKKU 1/2558).

CCA cell lines

CCA cell lines including KKU-055, KKU-100, KKU-213A, and KKU-213B were established from CCA patients under the Cholangiocarcinoma Research Institute, Faculty of Medicine, Khon Kaen University, Thailand. Each cell line was derived from different histological types of primary tumors from Thai CCA patients. Specifically, KKU-055 and KKU-100 originated from poorly differentiated adenocarcinoma, whereas KKU-213A and KKU-213B were derived from well-differentiated and moderately well-differentiated CCA, respectively[38]. All cells were cultured in DMEM high glucose medium supplemented with 10% fetal bovine serum (FBS; Gibco, NY) and 1% antibiotic–antimycotic (Gibco, NY) in a humidified incubator at 37 °C with 5% CO_2.

Lectin-histochemistry

Determination of ALAG expression in CCA patients and CCA-induced hamster tissues was performed by lectin-histochemistry as previously described[26]. Tissue sections were deparaffinized and rehydrated using gradient ethanol. Antigen retrieval was performed by boiling the sections in 0.1 M citrate buffer (pH 6.0) for 3 min. To neutralize endogenous peroxidase, sections were treated with 0.3% H_2O_2 in absolute methanol for 30 min. Non-specific binding was blocked by incubating the sections with 3% BSA in 1xPBS for 1 h. The sections were then incubated with biotinylated ALA (10 µg/mL) for 2 h, followed by 1:500 dilution of horseradish peroxidase (HRP)-conjugated streptavidin (Invitrogen, Camarillo, CA) for 1 h. Visualization was achieved using diaminobenzidine tetrahydrochloride (Abcam plc Inc. Cambridge, UK), and the sections were counterstained with Mayer's hematoxylin (Bio-Optica, Milan, Italy). Tissues were dehydrated in increasing ethanol concentrations, cleared with xylene, and mounted medium (Bio-Optica, Milan, Italy).

Lectin-cytofluorescent staining

ALAG expression in CCA cell lines was determined by lectin-cytofluorescence as previously described[27]. CCA cell lines (2×10^3 cells/well) were cultured in a 48-well plate for 72 h. Cells were fixed using absolute methanol for permeabilized samples and 4% paraformaldehyde for non-permeabilized samples. To block non-specific binding, cells were incubated with 3% BSA in 1xPBS for 1 h. Cells were then incubated with 1 µg/mL biotinylated-ALA overnight at 4 °C, followed by three washes with 1xPBS. Alexa Fluor 488-conjugated streptavidin (1:500 dilution; Thermo Fisher Scientific, MA) was added and incubated at room temperature for 1 h. Nuclei were stained with Hoechst 33342 (1:10,000 dilution; Sigma Aldrich, St.Louis, MO), and staining patterns were observed under a fluorescence microscope. Fluorescence intensity was analyzed using ImageJ software.

The neutralization effect of ALA on lectin-cytofluorescence was evaluated using 10 µg/mL BSM (Merck KGaA, Darmstadt, Germany) and sugars 9.0×10^4 µg/mL (Gal, glucose, and GalNAc). Biotinylated-ALA (1 µg/mL) was pre-incubated with glycoprotein or sugars at room temperature for 30 min before conducting the lectin-cytofluorescent staining.

Cell aggregation

CCA cell lines (2×10^4 cells/well) were plated in a 96-well plate. Cells were treated with varying concentrations of ALA (0–70 µg/mL) in serum-free media and incubated at 37 °C with 5% CO_2. Cell aggregation was detected and analyzed under a microscope after 1, 6, 12, and 24 h of ALA treatment.

Proliferation assay

CCA cell lines (2×10^3 cells/well) were plated into a 96-well plate for 24 h. Cells were treated with ALA (0–30 µg/mL) and cultured for 24, 48, and 72 h in a 5% CO_2 incubator at 37 °C. After treatment, 10 µL of MTT reagent (Thermo Fisher Scientific, Waltham, MA) was added to each well to achieve a final concentration of 0.5 mg/mL, and cells were incubated for an additional 3 h. To dissolve the purple formazan crystals, 100 µL of dimethyl sulfoxide was added to each well and the absorbance was measured at 540 nm.

Cell proliferation marker, Ki-67, was detected after treatment with 10 µg/mL ALA for 24 h. Ki-67 expression was determined using immuno-cytofluorescence with Ki-67 antibody (1:500 dilution; Dako, Copenhagen, Denmark).

Colony formation assay

CCA cell lines (5×10^2 cells/well) were cultured in a 48-well plate for 24 h in a 5% CO_2 incubator at 37 °C. Cells were then treated with ALA (0 to 20 µg/mL) for 7 days with media containing ALA replaced every three days. After treatment, cells were washed with 1xPBS and fixed with 4% paraformaldehyde for 20 min. Following staining with 0.5% crystal violet for 20 min, the cells were washed with distilled water until the background color was clear. The cell colonies were counted under a microscope, with each colony consisting of at least 50 cells.

Cell migration and invasion assay

Cell migration assay was performed using Transwell chambers (8 µm pore size, 24-well format) (Corning Incorporated, Corning, NY). For cell invasion assay, chambers were coated with 0.4 mg/mL Matrigel (Corning Incorporated, Corning, NY) and incubated overnight at 37 °C. CCA cell lines (1.5×10^5 cells/well) were cultured in a 6-well plate and treated with ALA (0–2 µg/mL) at 37 °C for 24 h in a 5% CO_2 incubator. After treatment, cells were placed in the upper chamber with the lower chamber containing a medium with 10% FBS. All cells

that migrated or invaded the underside of the membrane were fixed, stained with crystal violet, and counted in four random fields of view. Mean values were calculated from three independent experiments.

Gelatin zymography

Cells (5×10^4 cells/well) were cultured in a 24-well plate and treated with ALA (0–2 μg/mL) for 24 h. The culture media containing ALA was then replaced with serum-free DMEM high glucose media (Gibco, NY), and incubated for an additional 24 h. The conditioned medium was collected for zymogram analysis[39]. Electrophoresis was performed on a 10% polyacrylamide gel containing 1 mg/mL gelatin at 4 °C. The PAGE gels were run at 30 mA and 300 V. The gels were then incubated with renaturing buffer (2.5% Triton X-100 in 50 mM Tris–HCl, pH 7.4, 5 mM $CaCl_2$, 1 μM $ZnCl_2$, 0.01% NaN_3) for 1 h, followed by incubation with developing buffer (50 mM Tris–HCl, pH 7.4, 5 mM $CaCl_2$, 1 μM $ZnCl_2$, 0.01% NaN_3) at 37 °C overnight. Finally, the gels were stained with Coomassie Blue R-250 (USB Corporation, Cleveland) for 30 min and destained with destaining buffer until clear bands were visible.

Statistical analysis

Statistical analyses were performed using SPSS Statistics 28.0 software (SPSS, Inc.; Chicago, IL), and graphs were generated using GraphPad Prism 8 (GraphPad Inc., La Jolla, CA). ALAG expression levels in CCA tissues and cell lines were expressed as means with standard deviations (SD). Differences in ALAG expression levels between groups were assessed with Student's t-test. The correlation between ALA levels and clinicopathological data of CCA patients was analyzed using a Chi-square ($\chi2$) test. Additionally, Pearson correlation was employed to evaluate the relationship between ALA expression levels and continuous variables such as sex, age, tumor size, and tumor stage. Survival analysis was performed using Kaplan–Meier plots and Log-rank tests. A Cox proportional-hazards regression analysis was used to determine the hazard ratio (HR) and conduct multivariate survival analysis, selecting variables from the univariate Cox regression for inclusion. $P<0.05$ was considered statistically significant.

Data availability

The data and materials presented in this study are available on request from the corresponding author.

Received: 23 September 2024; Accepted: 23 December 2024
Published online: 02 January 2025

References

1. Sithithaworn, P., Yongvanit, P., Duenngai, K., Kiatsopit, N. & Pairojkul, C. Roles of liver fluke infection as risk factor for cholangiocarcinoma. *J. Hepatobiliary Pancreat. Sci.* **2**, 301–308 (2014).
2. Sripa, B. et al. Liver fluke induces cholangiocarcinoma. *PLoS Med.* **4**, 1148–1155 (2007).
3. Sivanand, A., Talati, D., Kalariya, Y., Patel, P. & Gandhi, S. K. Associations of liver fluke infection and cholangiocarcinoma: A scoping review. *Cureus* **15**, 1–6 (2023).
4. Banales, J. M. et al. Cholangiocarcinoma 2020: The next horizon in mechanisms and management. *Nat. Rev. Gastroenterol. Hepatol.* **17**, 557–588 (2020).
5. Brindley, P. J. et al. Cholangiocarcinoma. *Nat. Rev. Dis. Primers* **7**, 1–17 (2021).
6. Wu, H.-J. & Chu, P.-Y. Role of cancer stem cells in cholangiocarcinoma and therapeutic implications. *Int. J. Mol. Sci.* **20**, 4154 (2019).
7. de Souza-Ferreira, M., Ferreira, É. E. & de Freitas-Junior, J. C. Aberrant N-glycosylation in cancer: MGAT5 and β1,6-GlcNAc branched N-glycans as critical regulators of tumor development and progression. *Cell. Oncol.* **46**, 481–501 (2023).
8. Meany, D. L. & Chan, D. W. Aberrant glycosylation associated with enzymes as cancer biomarkers. *Clin. Proteom.* **8**, 7 (2011).
9. Wang, M., Zhu, J., Lubman, D. M. & Gao, C. Aberrant glycosylation and cancer biomarker discovery: A promising and thorny journey. *Clin. Chem. Lab. Med.* **57**, 407–416 (2019).
10. De-Freitas-Junior, J., Andrade-da-Costa, J., Silva, M. & Pinho, S. Glycans as regulatory elements of the insulin/IGF system: Impact in cancer progression. *Int. J. Mol. Sci.* **18**, 1921 (2017).
11. Gomes, C. et al. Expression of ST3GAL4 leads to SLex expression and induces c-Met activation and an invasive phenotype in gastric carcinoma cells. *PLoS ONE* **8**, e66737 (2013).
12. Ohtsubo, K. & Marth, J. D. Glycosylation in cellular mechanisms of health and disease. *Cell* **126**, 855–867 (2006).
13. Rodrigues, J. G. et al. Glycosylation in cancer: Selected roles in tumour progression, immune modulation and metastasis. *Cell. Immunol.* **333**, 46–57 (2018).
14. Very, N., Lefebvre, T. & el Yazidi-Belkoura, I. Drug resistance related to aberrant glycosylation in colorectal cancer. *Oncotarget* **9**, 1380–1402 (2018).
15. Zhao, H. et al. *N*-Glycosylation affects the adhesive function of E-Cadherin through modifying the composition of adherens junctions (AJs) in human breast carcinoma cell line MDA-MB-435. *J. Cell. Biochem.* **104**, 162–175 (2008).
16. Costa, A. F., Campos, D., Reis, C. A. & Gomes, C. Targeting glycosylation: A new road for cancer drug discovery. *Trends Cancer* **6**, 757–766 (2020).
17. da Costa, V. et al. Lung tumor cells with different Tn antigen expression present distinctive immunomodulatory properties. *Int. J. Mol. Sci.* **23** (2022).
18. Danese, E., Ruzzenente, A., Montagnana, M. & Lievens, P.M.-J. Current and future roles of mucins in cholangiocarcinoma—Recent evidences for a possible interplay with bile acids. *Ann. Transl. Med.* **6**, 333–333 (2018).
19. Dombek, G. E. et al. Immunohistochemical analysis of Tn antigen expression in colorectal adenocarcinoma and precursor lesions. *BMC Cancer* **22** (2022).
20. Ju, T., Aryal, R. P., Kudelka, M. R., Wang, Y. & Cummings, R. D. The Cosmc connection to the Tn antigen in cancer. *Cancer Biomark.* **14**, 63–81 (2014).
21. Matsumoto, Y., Jia, N., Heimburg-Molinaro, J. & Cummings, R. D. Targeting Tn-positive tumors with an afucosylated recombinant anti-Tn IgG. *Sci. Rep.* **13** (2023).
22. Rajesh, C. & Radhakrishnan, P. The (Sialyl) Tn antigen: Contributions to immunosuppression in gastrointestinal cancers. *Front. Oncol.* **12** (2023).
23. Kinzler, M. N. et al. Expression of MUC16/CA125 is associated with impaired survival in patients with surgically resected cholangiocarcinoma. *Cancers.* **14** (2022).

24. Sasaki, M., Yamato, T. & Nakanuma, Y. Expression of sialyl-Tn, Tn and T antigens in primary liver cancer. *Pathol. Int.* **49**(4), 325–331 (1999).
25. Mishra, A. et al. Structure-function and application of plant lectins in disease biology and immunity. *Food Chem. Toxicol.* **134** (2019).
26. Indramanee, S., Silsirivanit, A., Pairojkul, C., Wongkham, C. & Wongkham, S. Aberrant glycosylation in cholangiocarcinoma demonstrated by lectin-histochemistry. *Asian Pac. J. Cancer Prev.* **13**, 119–124 (2012).
27. Detarya, M. et al. The O-GalNAcylating enzyme GALNT5 mediates carcinogenesis and progression of cholangiocarcinoma via activation of AKT/ERK signaling. *Glycobiology* **30**, 312–324 (2020).
28. Detarya, M. et al. Emerging roles of GALNT5 on promoting EGFR activation in cholangiocarcinoma: A mechanistic insight. *Am. J. Cancer Res.* **12**, 4140–4159 (2022).
29. Wongkham, S. et al. Isolectins from seeds of *Artocarpus lakoocha*. *Phytochemistry* **40**, 1331–1334 (1995).
30. Singh, T., Chatterjee, U., Wu, J. H., Chatterjee, B. P. & Wu, A. M. Carbohyrate recognition factors of a Tα (Galβ1→3GalNAcα1→Ser/Thr) and Tn (GalNAcα1→Ser/Thr) specific lectin isolated from the seeds of *Artocarpus lakoocha*. *Glycobiology* **15**, 67–78 (2005).
31. Chatterjee, U., Bose, P. P., Dey, S., Singh, T. P. & Chatterjee, B. P. Antiproliferative effect of T/Tn specific *Artocarpus lakoocha* agglutinin (ALA) on human leukemic cells (Jurkat, U937, K562) and their imaging by QD-ALA nanoconjugate. *Glycoconj. J.* **25**, 741–752 (2008).
32. Springer, G. F. Immunoreactive T and Tn epitopes in cancer diagnosis, prognosis, and immunotherapy. *J. Mol. Med.* **75**, 594–602 (1997).
33. Wongkham, S. et al. Serum MUC5AC mucin as a potential marker for cholangiocarcinoma. *Cancer Lett.* **195**, 93–99 (2003).
34. Tollefsen, S. E. & Kornfeld, R. The B4 lectin from *Vicia villosa* seeds interacts with N-acetylgalactosamine residues alpha-linked to serine or threonine residues in cell surface glycoproteins. *J. Biol. Chem.* **258**, 5172–5176 (1983).
35. Chambers, A. F. & Matrisian, L. M. Changing views of the role of matrix metalloproteinases in metastasis. *J. Natl. Cancer Inst.* **89**, 1260–1270 (1997).
36. Laemmli, U. K. Cleavage of structural proteins during the assembly of the head of bacteriophage T4. *Nature* **227**, 680–685 (1970).
37. Prakobwong, S. et al. Involvement of MMP-9 in peribiliary fibrosis and cholangiocarcinogenesis via Rac1-dependent DNA damage in a hamster model. *Int. J. Cancer* **127**, 2576–2587 (2010).
38. Sripa, B. et al. Establishment and characterization of an opisthorchiasis-associated cholangiocarcinoma cell line (KKU-100). *World J. Gastroenterol.* **11**, 3392–3397 (2005).
39. Ren, Z., Chen, J. & Khalil, R. A. Zymography as a research tool in the study of matrix metalloproteinase inhibitors. *Methods Mol. Biol.* **1626**, 79–102 (2017).

Acknowledgements

We acknowledge the Cholangiocarcinoma Research Institute for providing CCA cell lines and tissues.

Author contributions

P.S. participated in the investigation, methodology, and statistical analysis under the supervision of K.V., P.M., A.S., S.W., and S.L., and contributed to writing the original draft. C.P. and C.A. participated in the histologic evaluation. U.C., K.V., and S.S. provided tissue samples or materials. A.S. participated in methodology, and statistical analysis and supervised the work. P.M. supervised the work. S.W. supervised the work and contributed to writing the manuscript. S.L. conceptualized and supervised the work, participated in the investigation, and contributed to writing, reviewing, and editing the manuscript. All authors reviewed the manuscript.

Funding

This research was supported by the Fundamental Fund of Khon Kaen University (for S.L.). P.S. was supported by the Postgraduate Study Support Grant of the Faculty of Medicine, Khon Kaen University, Thailand.

Declarations

Competing interests

The authors declare no competing interests.

Additional information

Supplementary Information The online version contains supplementary material available at https://doi.org/10.1038/s41598-024-84444-7.

Correspondence and requests for materials should be addressed to S.L.